Ultrasound in Med. & Biol., Vol. 42, No. 7, pp. 1660–1670, 2016

0301-5629/$ - see front matter

http://dx.doi.org/10.1016/j.ultrasmedbio.2016.02.015

*Original Contribution*

# OPTIMAL ACQUISITION SETTINGS FOR SPECKLE TRACKING ECHOCARDIOGRAPHY–DERIVED STRAINS IN INFANTS: AN *IN VITRO* STUDY

Umael Khan,* Johannes Just Hjertaas,* Gottfried Greve,[†‡] and Knut Matre*

*Bergen Hypertension and Cardiac Dynamics Group, Department of Clinical Science, University of Bergen, Bergen, Norway; [†]Department of Clinical Science, University of Bergen, Bergen, Norway; and [‡]Department of Heart Disease, Haukeland University Hospital, Bergen, Norway

(*Received* 25 *September* 2015; *revised* 2 *February* 2016; *in final form* 21 *February* 2016)

**Abstract—The purpose of this study was to investigate the effect of frame rate and probe frequency on the accuracy of speckle tracking echocardiography–derived strain measurements in infants. An infant-sized left ventricle phantom with sonomicrometer crystals was made from polyvinyl alcohol. The examined stroke rates were 60, 120 and 180 strokes per min (SPM). Longitudinal strain and circumferential strain measurements were analyzed from a total of 1860 cine loops. These cine loops were acquired using two pediatric probes of different frequencies at both fundamental and harmonic imaging modes. Both probes were examined at different settings (in total, 30 different frame rate–frequency combinations). At optimal settings, both longitudinal and circumferential strain displayed high accuracy. Frequency settings did not have a consistent effect on accuracy, while low frame rates led to less accurate measurements. We recommend a frame rate/heart ratio >1 frame per second/beats per min, especially for circumferential strain. (E-mail: knut.matre@uib.no) © 2016 World Federation for Ultrasound in Medicine & Biology.**

*Key Words:* **Myocardial strain, Infant, Phantom, *In vitro*, Frame rate, Frequency, Speckle tracking, Echocardiography, Sonomicrometer, Left ventricle.**

## INTRODUCTION

Myocardial strain is a new parameter for evaluation of left ventricular function, and longitudinal strain (LS) is included in the new clinical guidelines for chamber quantification for adults (Lang et al. 2015). Studies have also shown that strain is a useful echocardiographic parameter when assessing left ventricular function in infants (Al-Biltagi et al. 2015; Czernik et al. 2013; El-Khuffash et al. 2014; Nestaas et al. 2011). It can be obtained by speckle tracking echocardiography (STE) (Mondillo et al. 2011). However, STE in infants is challenging due to high heart rates combined with small heart size (Forsey et al. 2013). Therefore, there is a need for an investigation into how STE acquisition settings can be optimized for this age group.

Two important ultrasound acquisition settings are frame rate and frequency. The role of frame rate in STE measurements has been investigated in adults, children and infants (Rösner et al. 2015; Sanchez et al. 2015; Singh et al. 2010). These studies indicate that optimal frame rate depends on heart rate, implying that optimal frame rates for infants are higher than for adults (typically 40–70 frames per second [FPS]) (Dandel and Hetzer 2009). When assessing STE strains at different acquisition settings, if one is to examine the accuracy of STE strain measurements, a reference method is needed. One could examine agreement with magnetic resonance imaging measurements (Singh et al. 2010), but this is not suitable in non-anesthetized infants. This study examined strain in an infant-sized ventricular phantom using sonomicrometry as the reference method (Hjertaas et al. 2013).

There are few investigations into the impact of probe frequency and the use of harmonic imaging on STE strain accuracy in infants. A previous study using tissue Doppler imaging examined the role of probe frequency and concluded that increased probe frequency had a negative effect on the reproducibility of strain measurements (Nestaas et al. 2008).

The aim of this study is to examine the effect of frame rate, probe frequency and the use of harmonic imaging on the accuracy of both LS and circumferential strain (CS) measurements using speckle tracking in an infant-sized phantom.

Address correspondence to: Knut Matre, Bergen Hypertension and Cardiac Dynamics Group, Department of Clinical Science, University of Bergen, NO-5021 Bergen, Norway. E-mail: knut.matre@uib.no

## METHODS

*Ventricular phantom*

An infant-sized left ventricular phantom was made from a mixture of 10% polyvinyl alcohol (PVA) and 90% water (weight fractions). Sonomicrometer crystals (0.7 mm, Sonometrics Corporation, Ontario, Canada) were connected to a digital sonomicrometer (DS3-8, Sonometrics Corporation) and inserted into the phantom wall at mid-wall level (Figs. 1a and 1b). The phantom was connected to a pump that allowed us to regulate both stroke rate and stroke volume. Note that when discussing the pump, we use the terms *stroke*, *stroke rate* and *strokes per min* (SPM), whereas when discussing patients we use the terms *beats*, *heart rate* and *beats per min* (BPM). A more detailed description of the phantom production as well as the pump can be found in a previous publication from our group (Hjertaas et al. 2013).

The examined stroke rates were 60, 120 and 180 SPM. For each stroke rate a range of stroke volumes was applied in order to obtain a range of strain values. For examination of LS at stroke rates of 60 and 120 SPM, the stroke volume range was 3–25 mL (1-mL intervals). At a stroke rate of 180 SPM, the upper volume limit was 15 mL since the pump was unable to handle high stroke volumes at high stroke rates. Stroke volumes <3 mL were not included when examining LS, as the deformation was too small to be tracked by the STE software. For CS, the stroke volume range was 1–25 mL at stroke rates 60 and 120 SPM and 1–15 mL at stroke rate 180 SPM.

*Speckle tracking measurements*

For each setting of stroke rate and stroke volume, B-mode cine loops were obtained at a range of frame rate and frequency settings. Two pediatric cardiac probes of different frequencies were used, namely a 6 MHz probe (6 S) and a 12 MHz probe (12 S) using a digital scanner (Vivid E9, GE Vingmed Ultrasound, Horten, Norway). Figures 2a and 2b show the different settings for frequency and frame rate for both LS and CS measurements that were used. Initially, the default frequency settings for the neonate application of the scanner (9 MHz for the 12 S probe and 8 MHz for the 6 S probe) were used. Then, we switched to harmonic imaging (5.5/11 MHz for the 12 S probe and 3.1/6.2 MHz for the 6 S probe). Finally, the 12 S probe was used at 12 MHz, which was the highest possible frequency. The highest possible frequency for the 6 S probe was the default frequency. At each frequency setting there were three available frame rates, which were all examined. Hence, for each stroke rate–stroke volume combination, 15 different acquisition settings for LS and for CS measurements were applied. In total, 1860 cine loops were recorded.

The image sector width and depth were kept constant at 65° and 7 cm for LS and 90° and 6 cm for CS in order to fit the phantom into the sector at all stroke volumes. Because these settings were different when measuring LS and CS, the frame rates were also slightly different (Figs. 2a and 2b).

The ultrasound beam focal point (single focus) was visually adjusted to the depth of the sonomicrometer crystals for each view. The other settings for image acquisition were kept at the default settings for the preset neonate application mode. For the 12 S probe these were: compress = 11, reject = 10, dynamic range = 6. For the 6 S probe the settings were: compress = 12, reject = 2 and dynamic range = 6.

The cine loops were analyzed with EchoPac BT13 (GE Vingmed Ultrasound). LS was assessed in the 4-chamber speckle tracking mode and CS in the short axis papillary muscle speckle tracking mode. The inner border

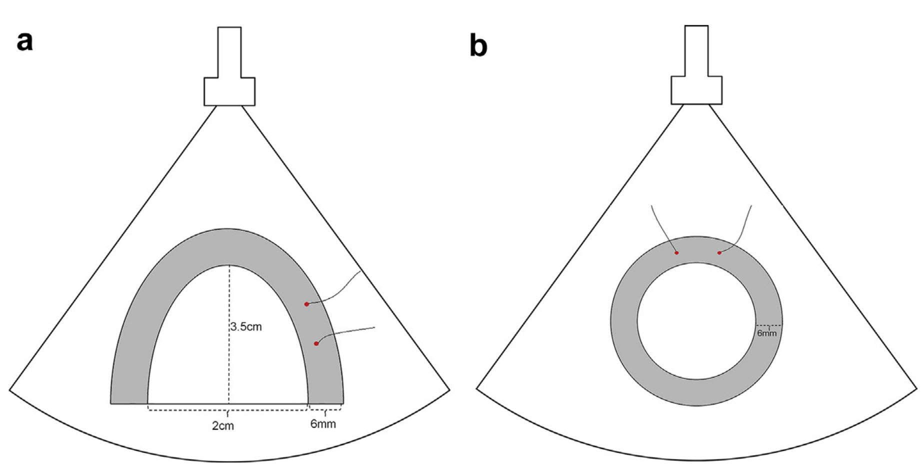


Fig. 1. Cross-sectional schematic views of the left ventricular phantom with dimensions at rest ("systole"). The red dots indicate the implanted sonomicrometer crystals. (a) Apical view for longitudinal strain measurements. (b) Short axis view for circumferential strain measurements. The ultrasound image depth and sector boundaries are indicated.

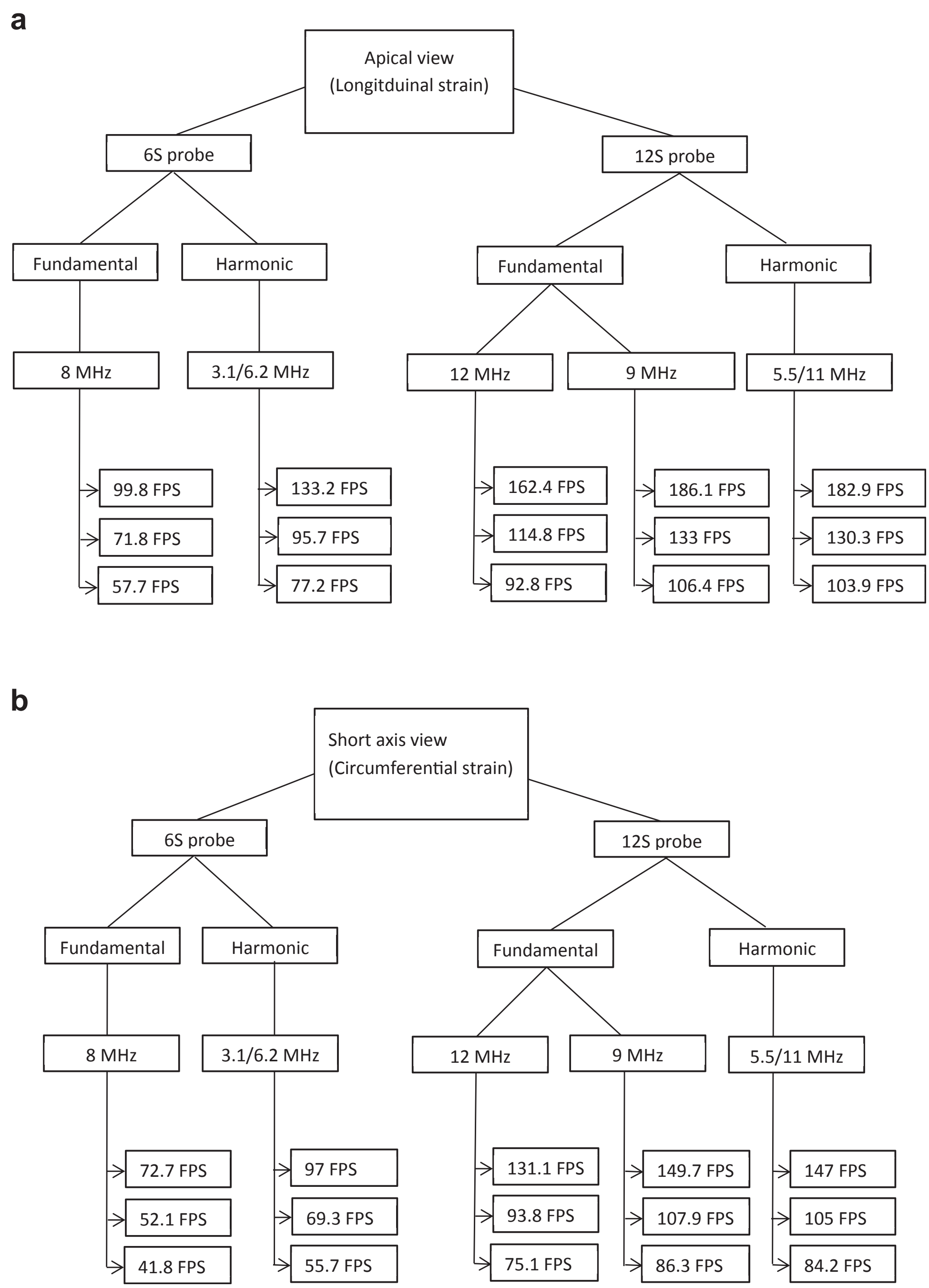


Fig. 2. Examined acquisition settings. Both fundamental and harmonic imaging were examined. At each frequency setting three different frame rates were tested. Hence, 15 acquisition settings were examined for measurements of longitudinal strain and 15 settings for circumferential strain. (a) Apical view (longitudinal strain). (b) Short axis view (circumferential strain). FPS = frames per second.

of the phantom wall was traced and the thickness of the region of interest adjusted to cover the phantom wall (Fig. 3). Segmental strain values were acquired from the segments, which included the sonomicrometer crystals.

In order to calculate intra-observer variability for STE strain, 20 random apical view B-mode cine loops and 20 short axis view B-mode cine loops were chosen 4 wk after the initial analysis and re-analyzed by the same observer (U.K.). The intra-class correlation coefficient was calculated. Inter-observer variability was assessed the same way except a second observer (J.H.) carried out the second analyses of the same 40 cine loops.

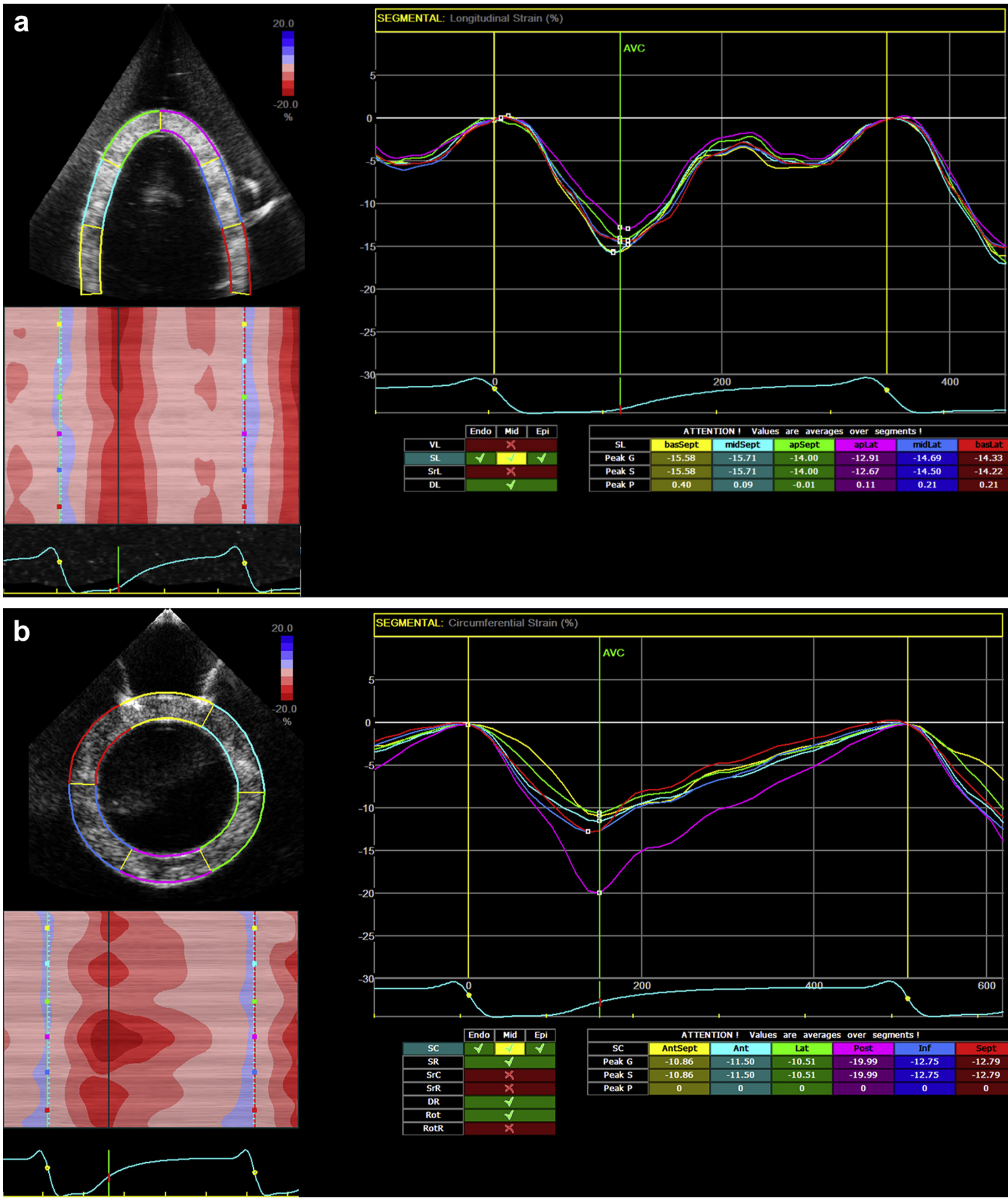


Fig. 3. Speckle tracking echocardiography using EchoPac BT13 (GE Vingmed Ultrasound). In both (a) and (b), the top left panels show the B-mode images each with six segments, the bottom left panels show the color strain maps and the right panels show the strain time curves with pump "electrocardiogram" and peak segmental strain values. (a) Measurement of longitudinal strain using the 12 S probe. (b) Measurement of circumferential strain using the 6 S probe.

*Sonomicrometer measurements*

In addition to obtaining B-mode cine loops at different acquisition settings, sonomicrometer measurements were also assessed at each stroke rate–stroke volume setting. The data from the sonomicrometer measurements were saved using commercial software (Sonolab; Sonometrics Corporation, Ontario, Canada). The distance between the sonomicrometer crystals was logged in Sonosoft (Sonometrics Corpration). The strain value was calculated by subtracting minimum distance between the crystals from the maximum distance, and dividing this by the maximum distance.

It was not possible to obtain sonomicrometer measurements and B-mode images simultaneously due to interference between the two acoustic signals. Instead, they were obtained from successive beats at each stroke rate–stroke volume setting. In order to avoid the effect of any changes in stroke volume during this procedure, sonomicrometer measurements were obtained from different beats at regular intervals. The closest recording in time to a particular B-mode recording was used for comparison.

*Statistics*

Accuracy of STE derived strain measurements was defined as the agreement with sonomicrometer derived strain measurements. At each stroke rate, we had a range of strain measurements (due to the stroke volume range) at different acquisition settings. The range of strain values at a particular stroke rate and acquisition setting was defined as a series. For each series, accuracy was assessed by Bland-Altman analyses of agreement between STE strain and sonomicrometer strain (Bland and Altman 1999). In addition, Pearson correlation coefficients between STE and sonomicrometer strain were also calculated.

The statistics was carried out using Microsoft Excel 2010 (Microsoft Corporation, Redmond, WA, USA) and SPSS Statistics 22 (SPSS Inc., Chicago, IL, USA), and the plots were drawn using SPSS and SigmaPlot 10.0 (SYSTAT Software, San Jose, CA, USA).

## RESULTS

As a summary of all the measurements, Table 1 and 2 show the correlation coefficients for all measurements series, while Figure 4 shows the results of the Bland-Altman analysis for all series. In general, low frame rates corresponded to less accurate strain measurements, this effect being more pronounced for CS than LS (Fig. 4). This is further illustrated in Figure 5, which shows complete scatter plots and Bland-Altman plots for two different frame rates for LS measurement (Figs. 5a and 5b) and for CS (Figs. 5c and 5d). Table 3 shows that optimal frame rate/stroke rate ratios when measuring LS were 1.4 and 0.7 for 120 and 180 SPM. For CS measurements, optimal frame rate at these stroke rates was the highest examined frame rate (149.7 FPS).

Increasing stroke rate did not have a large impact on the accuracy of the strain measurements at optimal acquisition settings. In fact, some of the least accurate CS measurements were obtained at stroke rate 60 SPM at low frame rates (Fig. 4).

Figure 4 also shows that neither increasing the frequency from 9 MHz to 12 MHz with the 12 S probe nor selecting harmonic imaging had a consistent impact on the accuracy of the strain measurements (both CS and LS). The 12 S probe offered higher frame rates than the 6 S probe. This generally corresponded to more accurate measurements with the 12 S probe. This was not seen for LS at stroke rate 60 SPM and 180 SPM, where the most accurate measurements were obtained with the 6 S probe (Table 3).

The intra-observer intra-class correlation coefficient was 0.999 for LS and 0.956 for CS, while the corresponding inter-observer intra-class correlation coefficient was 0.998 and 0.987.

Tracking quality was excellent for nearly all recordings. However, a combination of high stroke volumes and

Table 1. Correlation coefficients between STE-derived strains and sonomicrometry-derived strains for the 12 S probe at different stroke rates

| Strain direction | Frequency (MHz) | FR (FPS) | Correlation coefficient* | | |
|---|---|---|---|---|---|
| | | | 60 SPM | 120 SPM | 180 SPM |
| Longitudinal strain | 12.0 | 162.4 | 0.996 | 0.998 | 0.992 |
| | 12.0 | 114.8 | 0.993 | 0.996 | 0.995 |
| | 12.0 | 92.8 | 0.986 | 0.993 | 0.993 |
| | 9.0 | 186.1 | 0.998 | 0.997 | 0.993 |
| | 9.0 | 133.0 | 0.996 | 0.996 | 0.995 |
| | 9.0 | 106.4 | 0.998 | 0.990 | 0.990 |
| | 5.5/11 | 182.9 | 0.998 | 0.998 | 0.997 |
| | 5.5/11 | 130.3 | 0.980 | 0.996 | 0.996 |
| | 5.5/11 | 103.9 | 0.996 | 0.990 | 0.993 |
| Circumferential strain | 12.0 | 131.1 | 0.996 | 0.995 | 0.985 |
| | 12.0 | 93.8 | 0.993 | 0.971 | 0.931 |
| | 12.0 | 75.1 | 0.988 | 0.948 | 0.886 |
| | 9.0 | 149.7 | 0.994 | 0.997 | 0.978 |
| | 9.0 | 107.9 | 0.995 | 0.975 | 0.923 |
| | 9.0 | 86.3 | 0.992 | 0.922 | 0.860 |
| | 5.5/11 | 147.0 | 0.988 | 0.991 | 0.976 |
| | 5.5/11 | 105.0 | 0.981 | 0.972 | 0.944 |
| | 5.5/11 | 84.2 | 0.988 | 0.954 | 0.964 |

FR = frame rate; FPS = frames per second; SPM = strokes per min (stroke rate); STE = speckle tracking echocardiography.

* Pearson correlation coefficient between STE and sonomicrometry strain.

Table 2. Correlation coefficients between STE-derived strains and sonomicrometry-derived strains for the 6 S probe at different stroke rates

| Strain direction | Frequency (MHz) | FR (FPS) | Correlation coefficient* | | |
|---|---|---|---|---|---|
| | | | 60 SPM | 120 SPM | 180 SPM |
| Longitudinal strain | 8 | 99.8 | 0.996 | 0.991 | 0.996 |
| | 8 | 71.8 | 0.993 | 0.984 | 0.993 |
| | 8 | 57.7 | 0.993 | 0.974 | 0.983 |
| | 3.1/6.2 | 133.2 | 0.999 | 0.973 | 0.996 |
| | 3.1/6.2 | 95.7 | 0.998 | 0.957 | 0.998 |
| | 3.1/6.2 | 77.2 | 0.996 | 0.961 | 0.987 |
| Circumferential strain | 8 | 72.7 | 0.991 | 0.857 | 0.885 |
| | 8 | 52.1 | 0.883 | 0.914 | 0.956 |
| | 8 | 41.8 | 0.917 | 0.949 | 0.863 |
| | 3.1/6.2 | 97.0 | 0.985 | 0.845 | 0.859 |
| | 3.1/6.2 | 69.3 | 0.760 | 0.861 | 0.751 |
| | 3.1/6.2 | 55.7 | 0.804 | 0.854 | 0.715 |

FR = frame rate; FPS = frames per second; SPM = strokes per min (stroke rate); STE = speckle tracking echocardiography.

* Pearson correlation coefficient between STE and sonomicrometry strain.

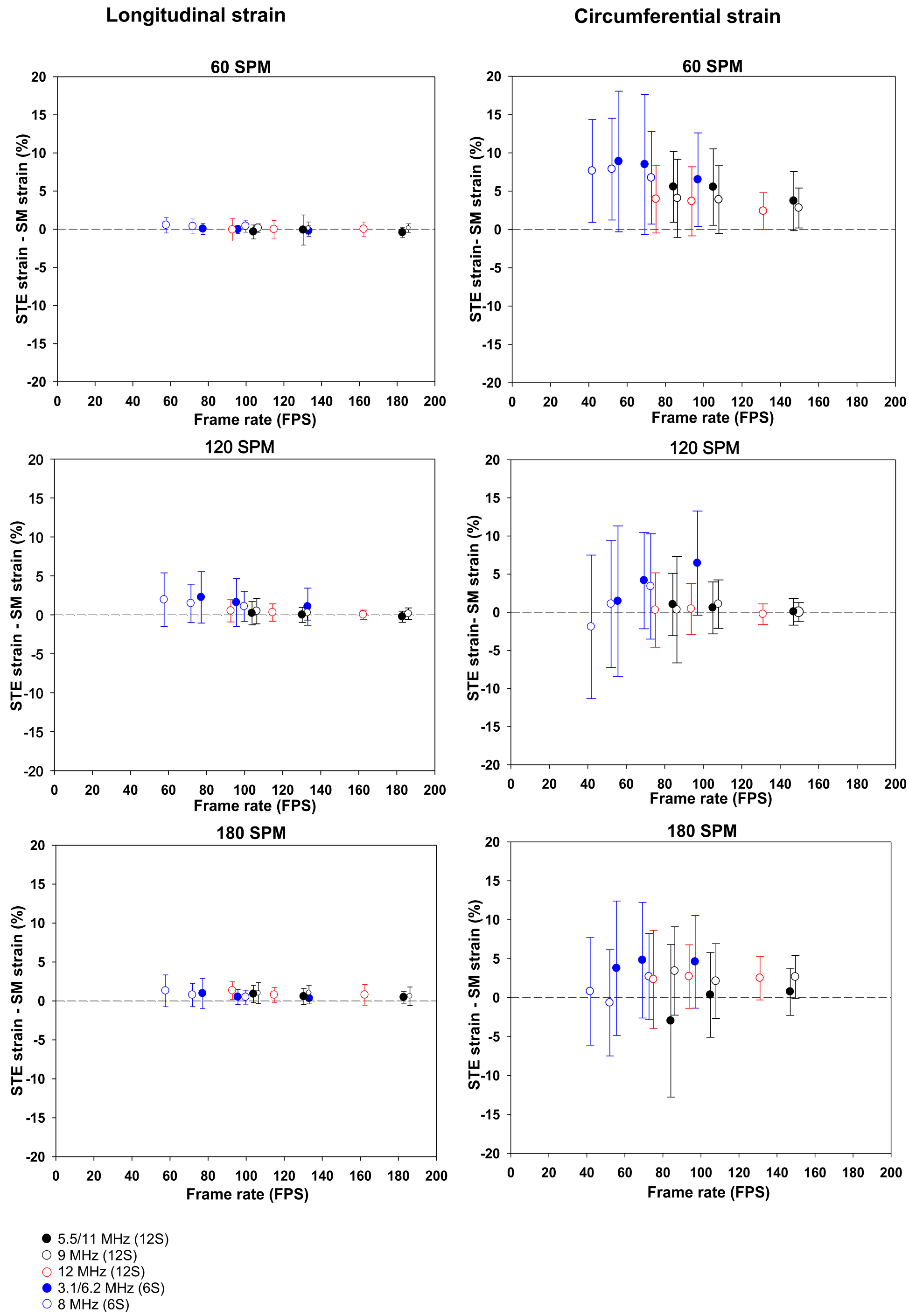


Fig. 4. Agreement between speckle tracking and sonomicrometry strains at different acquisition settings. Each point represents the mean difference between speckle tracking–derived strain and sonomicrometry-derived strain at a specific frame rate. The error bars are representing ± 2 standard deviations of this difference. Each point and error bars corresponds to a single Bland-Altman analysis and the error bars represent the limits of agreement of the difference. FPS = frames per second; SM = sonimicrometry; SPM = stroke per min (stroke rate); STE = speckle tracking echocardiography.

low frame rates led to faulty tracking when using the 6 S probe. Among the 1860 segments examined, three images were excluded due to faulty tracking of the segment with the crystals.

The resulting LS range was −3% to −16% at stroke rate 180 SPM and −3% to −19% at stroke rates 60 and 120 SPM. The corresponding CS ranges were −2% to −20% and −2% to −24%.

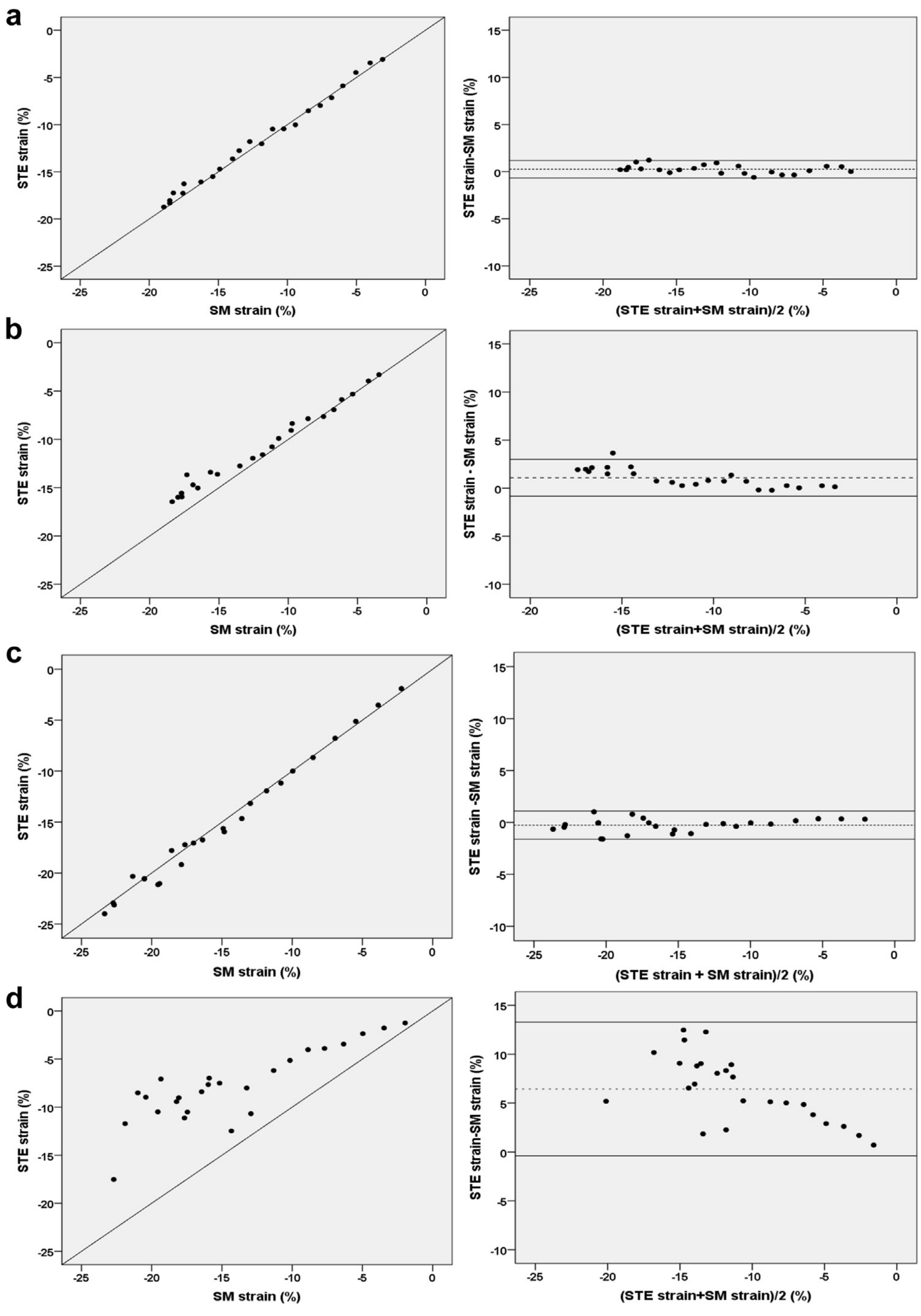


Fig. 5. Scatter plots with line of unity (left column) and Bland-Altman plots (right column) displaying agreement between sonomicrometry strains and STE strains for selected series at stroke rate 120 strokes per min. Longitudinal strain (LS) at frame rate 133 frames per second (FPS) (a); LS at frame rate 99.8 FPS (b); circumferential strain (CS) at frame rate 131.1 FPS (c); CS at frame rate 97 FPS (d). SM = sonimicrometry; STE = speckle tracking echocardiography.

## DISCUSSION

Our study shows that accurate LS and CS measurements can be obtained at optimal settings. CS was more dependent on acquisition settings than LS. Both LS and CS measurements show high reproducibility.

*Frame rate dependency*

Our results show a strong frame rate dependency of CS measurements at all three stroke rates. A possible explanation for this is the in and out of plane motion in short axis imaging. The phantom (or ventricle in an *in vivo* setting) will shift in and out of the imaging plane

Table 3. Optimal probe, probe settings and the resulting accuracy for LS and CS measurements at different stroke rates

| Optimal settings | 60 SPM | 120 SPM | 180 SPM |
|---|---|---|---|
| Longitudinal strain | | | |
| Probe | 6 S | 12 S | 6 S |
| Frequency | 3.1/6.2 | 12 | 3.1/6.2 |
| FR (FPS) | 95.7 | 162.4 | 133.2 |
| FR/SR (FPS/SPM) | 1.6 | 1.4 | 0.7 |
| Mean offset* | −0.03 | 0.01 | 0.33 |
| 2 SD† | 0.54 | 0.59 | 0.71 |
| Correlation coefficient‡ | 0.998 | 0.998 | 0.996 |
| Circumferential strain | | | |
| Probe | 12 S | 12 S | 12 S |
| Frequency | 12 | 9 | 9 |
| FR (FPS) | 131.1 | 149.7 | 149.7 |
| FR/SR (FPS/SPM) | 2.2 | 1.2 | 0,8 |
| Mean offset* | 2.44 | 0.01 | 2.65 |
| 2 SD† | 2.39 | 1.25 | 2.74 |
| Correlation coefficient‡ | 0.996 | 0.997 | 0.978 |

CS = circumferential strain; FPS = frames per second; FR = frame rate; FR/SR = frame rate/stroke rate ratio; LS = longitudinal strain; SD = standard deviation; SPM = strokes per minute (stroke rate).

* Mean offset between STE and sonomicrometry derived strain in %.

† Standard deviation of mean offset in %.

‡ Pearson correlation coefficient between STE and sonomicrometry strain.

during the contraction-relaxation cycle due to the elongation and contraction in the longitudinal direction. This will lead to a more rapidly changing speckle pattern. Since the basis for speckle tracking is the tracing of specular patterns (kernels) over successive frames (Leitman et al. 2004), this would lead to uncertainty in the strain algorithm. Based on this premise one would expect that a high frame rate is more important in order to track the kernels accurately during short axis imaging in comparison to long axis imaging, especially at a high stroke rate.

The optimal frame rate/stroke rate ratios for CS measurements (Table 3) are higher than the minimum ratio of 0.5 FPS/BPM that Rösner et al. (2015) recommended based on their combined *in silico*–adult study. It is closer to the result from the reproducibility analysis by Singh et al. (2010) in children, showing an optimal frame rate of 60–90 FPS for both LS and CS measurements when the average heart rate was 75 BPM. We were unable to increase the frame rate beyond 149.7 FPS for CS measurements due the necessary sector width and depth settings. Most scanners have a limitation in frame rate at a particular setting to avoid low beam density that will reduce the lateral resolution and thus the image quality. Given the high optimal frame rate/stroke rate ratio at stroke rate 60 SPM, it seems likely that the optimal frame rate/stroke rate ratio would be greater than what we found for stroke rates 120 and 180 SPM if no limitation of the frame rate due to beam density was present.

For LS measurements, Figure 4 indicates that the optimal frame rate/stroke rate ratio is around 1 FPS/SPM, which corresponds well to a recent study by Sanchez et al. (2015), showing an optimal frame rate/heart rate ratio above 0.7 FPS/BPM in preterm infants. At the same time, the robustness of LS measurements with regards to frame rate (Fig. 4) also indicates that a lower frame rate is acceptable. In fact, the most accurate strain measurements at stroke rate 180 SPM were obtained with the 6 S probe at frame rate 133.2 FPS (Table 3), while the second most accurate measurements were close and were obtained with the 12 S probe at frame rate 182.9 FPS. This also corresponds well with a previous reproducibility study in adults which found that a frame rate as low as 30 FPS was acceptable when measuring LS (but not CS) in adults (Risum et al. 2012). Furthermore, a meta-analysis of strain in adults did not find a significant inter-study association between frame rate and LS (Yingchoncharoen et al. 2013).

### *Frequency dependency*

When examining frequency settings for the two pediatric probes, the frequencies selected were the default frequencies for the "neonate" application as described under Methods and shown in Figure 2, as well as the highest harmonic frequencies. These were selected because we wanted to examine frequency settings that would typically be used for infants. We found that neither using harmonic imaging nor increasing in frequency from 9 MHz to 12 MHz affected the accuracy of strain measurements. However, the 12 S probe offered higher frame rates than the 6 S probe leading to more accurate strain measurements.

While no previous study has been carried out on the effect of frequency on STE accuracy in infants, a previous study investigated the effect of probe frequency on tissue Doppler imaging–derived strain in infants. It showed that increasing the Doppler frequency and frame rate using different probes led to nosier strain measurements. However, these results were only seen when comparing strain time curves rather than comparing peak strain values (Nestaas et al. 2008). When comparing peak strain values, they found no correlation between frame rate or frequency and the reproducibility of the strain measurements, a result that is similar to this study. However, it is important to note that tissue Doppler imaging and STE are fundamentally different echocardiographic deformation techniques, and the effect of probe frequency is likely to be different.

### *Previous studies*

Most studies in children and adults showed that LS measurements were more reproducible than CS measurements (Cho et al. 2006; Koopman et al. 2011; Risum et al. 2012; Singh et al. 2010). However, studies that assessed the accuracy of LS and CS showed more discrepancy.

A study in dogs using sonomicrometry as the reference method found that LS measurements with an adult probe were more accurate than CS measurements (Amundsen et al. 2006). Later studies, using magnetic resonance imaging as the reference method, have shown more variable results regarding relative accuracy of CS and LS, partly depending on ventricular geometry (Bansal et al. 2008; Cho et al. 2006; Singh et al. 2010). Our study shows a higher accuracy of LS compared to CS, especially at lower frame rates. This can partially be explained by the in and out of plane motion of the phantom in the short axis view, as discussed in the section on frame rate dependency above.

*Angle and depth dependency*

The segment we examined for CS was almost perpendicular to the beam direction, whereas the segment we examined for LS was almost parallel. Angle of insonation plays a role in STE strain measurements, possibly due to a lower lateral than axial resolution (Forsha et al. 2015). This should be kept in mind when comparing the relative accuracy of LS and CS. An important distinction between this study and several previous studies is that we have examined regional strain in the segment with the crystals, whereas previous studies present either global LS or global CS. Global LS and global CS include segments that are both parallel and perpendicular to the ultrasound beam.

Another aspect that should be mentioned is depth. Cardiac ultrasound probes are sector probes, and the ultrasound beams diverge from each other as they move away from the probe and results in a decreased lateral resolution at depth. A recent study showed that there was a systemic bias in strain measurements between myocardial segments placed on the near-field and far-field of the ultrasound beam (Forsha et al. 2015). Although it would have been interesting to examine the effect of strain from segments at different depths, this was not carried out because a direct comparison with the reference method was the key feature of this study and strain values were only read from segments with sonomicrometer crystals.

*Vendor dependency*

This study investigates the effect of acquisition settings using equipment from only one vendor. One of the challenges related to echocardiographic strain measurements has been inter-vendor differences (Marwick 2010). Although inter-vendor difference in strain values has been reduced in recent years (Yang et al. 2015), an important follow-up of this study would be to examine whether our findings are valid for different vendors.

*Experimental set-up*

This experiment was conducted using a ventricular phantom. In addition to using sonomicrometry as the reference method, further advantages of using this set-up are control and reproducibility. Strokes with different stroke volumes can be produced with precision using a pump attached to a stepping motor. On the other hand, a ventricular phantom does not include the same electrophysiological processes as an *in vivo* left ventricular contraction. For instance, deformation of the phantom is caused by passive elasticity rather than active contraction. However, strain measurement is a measure of deformation, irrespective of the underlying mechanism. *In vitro* set-ups are, therefore, suitable for the purpose of this experiment, and have been utilized in other pre-clinical investigations into the accuracy of strain measurements (Hjertaas et al. 2013; Sivesgaard et al. 2009). Nevertheless, there are some limitations that must be taken into consideration. First of all, the phantom was made from PVA. Despite the fact that it has been shown to be a suitable tissue substitute for ultrasound imaging (Culjat et al. 2010), it does not include the effect of myocardial fiber orientation on ultrasound backscatter (Aygen and Popp 1987).

In Figure 3b, the most posterior segment displays a higher strain than the other segments. This is most likely due to, in addition to uncertainty in the speckle tracking software, the fact that the phantom is not completely homogenous with regards to composition and elastic properties. This illustrated the importance of acquiring sonomicrometer-derived strain and speckle tracking–derived strain from the same segment. Acquiring them from different segments of the phantom could lead to inaccuracies in strain comparison that is due to phantoms heterogeneity. Furthermore, our set-up lacked a thoracic wall, which is a source of attenuation and reverberations in clinical imaging. This could have some influence on our results regarding harmonic imaging since harmonic imaging includes a reduction of reverberations.

The *in vitro* set-up introduced artifacts, most important of which were reverberations. We placed the phantom and crystals to avoid these reverberations. In addition, we also wanted to make sure the phantom was visible throughout the pump cycle. For this reason, the total image depth was 7 cm. This is a bit larger than the image depth one could have when examining infants (in a pilot study in infants we found this depth to be 4–5 cm). Although we do not consider this to be a large error, one should bear in mind that some scanners reduce the frame rate in response to increasing depth and that the lateral resolution is decreasing with depth for a sector probe. It is important to keep in mind that although the image depth was 7 cm, the beam focus was at the segment with crystals (approximately 4 cm from the probe in the long axis view and 2 cm from the probe in the short axis view), which is not very different compared to a clinical situation.

In this study, we used a higher pre-load than is normally found in infants. This was necessary in order to create sufficient elastic recoil in the phantom and start the filling at the correct geometry (Hjertaas et al. 2013). Hence, a stroke volume of 25 mL in this experimental setup would correspond to a lower stroke volume in infants. A study of normal values for left ventricular strain in infants has reported LS to be −16% in the middle lateral segment and CS to be −25% in the anterior septal segment (Marcus et al. 2011). Thus, we have obtained and examined both normal and sub-normal strain values in our experimental set-up.

While the use of adult sized left ventricular phantoms is well established (Heyde et al. 2012; Hjertaas et al. 2013; Lesniak-Plewinska et al. 2010; Mårtensson et al. 2011; Surry et al. 2004), to our knowledge, we are the first to use an infant-sized PVA phantom for assessing strain measurements using high frequency probes.

## CONCLUSIONS

Accurate strain measurements can be obtained at high heart rates when acquisition parameters are optimized. We recommend using pediatric probes that allow a frame rate/heart rate ratio above 1 FPS/BPM when measuring ventricular strain in infants. This is especially important for CS.

*Acknowledgments*—Financial support was obtained from the Bergen University Heart Foundation and from the MedViz consortium, an inter-institutionary research and development program in medical visualization by the University of Bergen, Haukeland University Hospital and Christian Michelsen Research.

## REFERENCES

Al-Biltagi M, Tolba OA, Rowisha MA, Mahfouz Ael S, Elewa MA. Speckle tracking and myocardial tissue imaging in infant of diabetic mother with gestational and pregestational diabetes. Pediatr Cardiol 2015;36:445–453.

Amundsen BH, Helle-Valle T, Edvardsen T, Torp H, Crosby J, Lyseggen E, Støylen A, Ihlen H, Lima JA, Smiseth OA, Slørdahl SA. Noninvasive myocardial strain measurement by speckle tracking echocardiography: Validation against sonomicrometry and tagged magnetic resonance imaging. J Am Coll Cardiol 2006;47:789–793.

Aygen M, Popp RL. Influence of the orientation of myocardial fibers on echocardiographic images. Am J Cardiol 1987;60:147–152.

Bansal M, Cho GY, Chan J, Leano R, Haluska BA, Marwick TH. Feasibility and accuracy of different techniques of two-dimensional speckle based strain and validation with harmonic phase magnetic resonance imaging. J Am Soc Echocardiogr 2008;21:1318–1325.

Bland JM, Altman DG. Measuring agreement in method comparison studies. Stat Methods Med Res 1999;8:135–160.

Cho GY, Chan J, Leano R, Strudwick M, Marwick TH. Comparison of two-dimensional speckle and tissue velocity based strain and validation with harmonic phase magnetic resonance imaging. Am J Cardiol 2006;97:1661–1666.

Culjat MO, Goldenberg D, Tewari P, Singh RS. A review of tissue substitutes for ultrasound imaging. Ultrasound Med Biol 2010;36: 861–873.

Czernik C, Rhode S, Helfer S, Schmalisch G, Buhrer C. Left ventricular longitudinal strain and strain rate measured by 2-D speckle tracking echocardiography in neonates during whole-body hypothermia. Ultrasound Med Biol 2013;39:1343–1349.

Dandel M, Hetzer R. Echocardiographic strain and strain rate imaging–clinical applications. Int J Cardiol 2009;132:11–24.

El-Khuffash AF, Jain A, Weisz D, Mertens L, McNamara PJ. Assessment and treatment of post patent ductus arteriosus ligation syndrome. J Pediatr 2014;165:46–52.e1.

Forsey J, Friedberg MK, Mertens L. Speckle tracking echocardiography in pediatric and congenital heart disease. Echocardiography 2013; 30:447–459.

Forsha D, Risum N, Rajagopal S, Dolgner S, Hornik C, Barnhart H, Kisslo J, Barker P. The influence of angle of insonation and target depth on speckle-tracking strain. J Am Soc Echocardiogr 2015;28: 580–586.

Heyde B, Cygan S, Choi HF, Lesniak-Plewinska B, Barbosa D, Elen A, Claus P, Loeckx D, Kaluzynski K, D'Hooge J. Regional cardiac motion and strain estimation in three-dimensional echocardiography: A validation study in thick-walled univentricular phantoms. IEEE Trans Ultrason Ferroelectr Freq Control 2012;59:668–682.

Hjertaas JJ, Fosså H, Dybdahl GL, Grüner R, Lunde P, Matre K. Accuracy of real-time single- and multi-beat 3-d speckle tracking echocardiography *in vitro*. Ultrasound Med Biol 2013;39: 1006–1014.

Koopman LP, Slorach C, Manlhiot C, McCrindle BW, Jaeggi ET, Mertens L, Friedberg MK. Assessment of myocardial deformation in children using Digital Imaging and Communications in Medicine (DICOM) data and vendor independent speckle tracking software. J Am Soc Echocardiogr 2011;24:37–44.

Lang RM, Badano LP, Mor-Avi V, Afilalo J, Armstrong A, Ernande L, Flachskampf FA, Foster E, Goldstein SA, Kuznetsova T, Lancellotti P, Muraru D, Picard MH, Rietzschel ER, Rudski L, Spencer KT, Tsang W, Voigt JU. Recommendations for cardiac chamber quantification by echocardiography in adults: An update from the American Society of Echocardiography and the European Association of Cardiovascular Imaging. J Am Soc Echocardiogr 2015;28:1–39.e14.

Leitman M, Lysyansky P, Sidenko S, Shir V, Peleg E, Binenbaum M, Kaluski E, Krakover R, Vered Z. Two-dimensional strain-a novel software for real-time quantitative echocardiographic assessment of myocardial function. J Am Soc Echocardiogr 2004;17: 1021–1029.

Lesniak-Plewinska B, Cygan S, Kaluzynski K, D'Hooge J, Zmigrodzki J, Kowalik E, Kordybach M, Kowalski M. A dual-chamber, thick-walled cardiac phantom for use in cardiac motion and deformation imaging by ultrasound. Ultrasound Med Biol 2010;36:1145–1156.

Marcus KA, Mavinkurve-Groothuis AM, Barends M, van Dijk A, Feuth T, de Korte C, Kapusta L. Reference values for myocardial two-dimensional strain echocardiography in a healthy pediatric and young adult cohort. J Am Soc Echocardiogr 2011;24: 625–636.

Mårtensson M, Bjallmark A, Brodin LA. Evaluation of tissue Doppler-based velocity and deformation imaging: a phantom study of ultrasound systems. Eur J Echocardiogr 2011;12:467–476.

Marwick TH. Consistency of myocardial deformation imaging between vendors. Eur J Echocardiogr 2010;11:414–416.

Mondillo S, Galderisi M, Mele D, Cameli M, Lomoriello VS, Zaca V, Ballo P, D'Andrea A, Muraru D, Losi M, Agricola E, D'Errico A, Buralli S, Sciomer S, Nistri S, Badano L. Speckle-tracking echocardiography: A new technique for assessing myocardial function. J Ultrasound Med 2011;30:71–83.

Nestaas E, Støylen A, Brunvand L, Fugelseth D. Longitudinal strain and strain rate by tissue Doppler are more sensitive indices than fractional shortening for assessing the reduced myocardial function in asphyxiated neonates. Cardiol Young 2011;21:1–7.

Nestaas E, Støylen A, Fugelseth D. Optimal types of probe, and tissue Doppler frame rates, for use during tissue Doppler recording and off-line analysis of strain and strain rate in neonates at term. Cardiol Young 2008;18:502–511.

Risum N, Ali S, Olsen NT, Jons C, Khouri MG, Lauridsen TK, Samad Z, Velazquez EJ, Søgaard P, Kisslo J. Variability of global left ventricular deformation analysis using vendor dependent and independent two-dimensional speckle-tracking software in adults. J Am Soc Echocardiogr 2012;25:1195–1203.

Rösner A, Barbosa D, Aarsaether E, Kjonas D, Schirmer H, D'Hooge J. The influence of frame rate on two-dimensional speckle-tracking strain measurements: A study on silico-simulated models and images recorded in patients. Eur Heart J Cardiovasc Imaging 2015;16:1137–1147.

Sanchez AA, Levy PT, Sekarski TJ, Hamvas A, Holland MR, Singh GK. Effects of frame rate on two-dimensional speckle tracking-derived measurements of myocardial deformation in premature infants. Echocardiography 2015;32:839–847.

Singh GK, Cupps B, Pasque M, Woodard PK, Holland MR, Ludomirsky A. Accuracy and reproducibility of strain by speckle tracking in pediatric subjects with normal heart and single ventricular physiology: A two-dimensional speckle-tracking echocardiography and magnetic resonance imaging correlative study. J Am Soc Echocardiogr 2010;23:1143–1152.

Sivesgaard K, Christensen SD, Nygaard H, Hasenkam JM, Sloth E. Speckle tracking ultrasound is independent of insonation angle and gain: an *in vitro* investigation of agreement with sonomicrometry. J Am Soc Echocardiogr 2009;22:852–858.

Surry KJ, Austin HJ, Fenster A, Peters TM. Poly (vinyl alcohol) cryogel phantoms for use in ultrasound and MR imaging. Phys Med Biol 2004;49:5529–5546.

Yang H, Marwick TH, Fukuda N, Oe H, Saito M, Thomas JD, Negishi K. Improvement in strain concordance between two major vendors after the strain standardization initiative. J Am Soc Echocardiogr 2015;28:642–648.e7.

Yingchoncharoen T, Agarwal S, Popovic ZB, Marwick TH. Normal ranges of left ventricular strain: A meta-analysis. J Am Soc Echocardiogr 2013;26:185–191.